CD40 stimulation sensitizes CLL cells to lysosomal cell death induction by type II anti-CD20 mAb GA101

Margot Jak,[1,2] Gregor G. W. van Bochove,[1] Eric A. Reits,[3] Wouter W. Kallemeijn,[4] Jacqueline M. Tromp,[1,2] Pablo Umana,[5] Christian Klein,[5] Rene A. W. van Lier,[2] Marinus H. J. van Oers,[1] and Eric Eldering[2]

Departments of [1]Hematology, [2]Experimental Immunology, [3]Cell Biology and Histology, and [4]Biochemistry, Academic Medical Centre, Amsterdam, The Netherlands; and [5]Pharma Research and Early Development, Roche Glycart AG, Schlieren, Switzerland

Sensitivity of chronic lymphocytic leukemia (CLL) cells to anti-CD20 mAbs is low and, therefore, the efficacy of monotherapy with current anti-CD20 mAbs is limited. At present, it is not known whether sensitivity of CLL cells to CD20 mAbs is modulated by microenvironmental stimuli. We have shown previously that in vitro CD40 stimulation of peripheral blood–derived CLL cells results in resistance to cytotoxic drugs. In the present study, we show that, in contrast, CD40 stimulation sensitizes CLL cells to the recently described novel type II anti-CD20 mAb GA101. Cell death occurred without cross-linking of GA101 and involved a lysosome-dependent mechanism. Combining GA101 with various cytotoxic drugs resulted in additive cell death, not only in CD40-stimulated CLL cells, but also in p53-dysfunctional CLL cells. Our findings indicate that GA101 has efficacy against chemoresistant CLL, and provide a rationale for combining cytotoxic drugs with anti-CD20 mAbs. (*Blood*. 2011;118(19): 5178-5188)

Introduction

Although treatment results for chronic lymphocytic leukemia (CLL) have improved considerably over the last decade, a curative drug regimen is still lacking. Similar to other B-cell malignancies such as follicular lymphoma and multiple myeloma, in CLL, the interaction of the malignant cells with their microenvironment in the lymph nodes, spleen, and possibly BM has been shown to play an important role in the biology of the disease.[1] We and others have previously shown that in vitro CD40 stimulation of CLL cells can to a certain extent mimic the lymph node environment and results in the induction of resistance of the CLL cells to cytotoxic drugs such as fludarabine, chlorambucil, bortezomib, and roscovitine.[2-6] These microenvironmental niches might be an important localization of minimal residual disease and form the basis for the relapses characterizing this disease.[1,3-5,7,8] Moreover, after sequential treatments, selection of p53 dysfunctional clones occurs in up to 50% of patients,[9,10] which also results in chemoresistance. Therefore, there is a need for new treatments that circumvent microenvironmental chemoresistance and act independently of p53, possibly including anti-CD20 mAb–containing regimens.[11,12] However, sensitivity of CLL cells to anti-CD20 mAbs in vitro is low and monotherapy with conventional doses of the type I anti-CD20 mAb rituximab has only limited efficacy in CLL. Because of rituximab resistance or unresponsiveness, more potent anti-CD20 mAbs are currently being sought. Two types of anti-CD20 mAbs have been described. A prime difference is that, in contrast to type I anti-CD20 mAbs, type II mAbs are unable to translocate CD20 into lipid rafts or to evoke Ca^{2+} flux.[13-16] Ofatumumab, a second-generation type I anti-CD20 mAb seems promising for the treatment of CLL,[17] although large amounts seem to be required. GA101 is a novel glycoengineered type II anti-CD20 mAb. Compared with rituximab, GA101 has enhanced direct cell death–inducing capacity and improved Ab-dependent cellular cytotoxicity.[15,18] GA101 was also more potent than rituximab at equivalent concentrations in depleting CLL cells in vitro.[19] Finally, a phase 1 study with GA101 in heavily pretreated relapsed/refractory CLL patients showed promising activity when given as single agent,[20] and recent studies showed that type II anti-CD20 mAbs induce homotypic adhesion-related cell death through a lysosome-dependent pathway.[21,22]

Rather unexpectedly, we recently found that, in contrast to its induction of chemoresistance, CD40 stimulation enhanced sensitivity of CLL cells to rituximab via a reactive oxygen species (ROS)–dependent mechanism.[23] Because of the largely different mechanism of action of type I compared with type II anti-CD20 mAbs, we investigated in the present study whether CD40 stimulation also affects the sensitivity of CLL cells to GA101 and, if so, by what mechanism.

Methods

Patient samples

Peripheral blood was drawn from CLL patients (diagnosed according to the National Cancer Institute Working Group guidelines). PBMCs were isolated by Ficoll density gradient centrifugation (Pharmacia Biotech), and were either used immediately or stored in liquid nitrogen. During all in vitro experiments, cells were maintained in the following culture medium: IMDM (GIBCO) supplemented with 10% heat-inactivated FCS, 100 U/mL of penicillin, 100 μg/mL of gentamycin, and 0.00036% β-mercaptoethanol. All samples contained at least 90% $CD5^+/CD19^+$ cells as assessed via flow cytometry. p53 dysfunction of patient samples was assessed with cytogenetics (del17p13) in combination with multiplex quantification of p53 target gene induction, as described previously.[24] The studies were approved by the ethical review board of the Academic Medical Centre in Amsterdam and

Submitted January 25, 2011; accepted September 3, 2011. Prepublished online as *Blood* First Edition manuscript, September 26, 2011; DOI: 10.1182/blood-2011-01-331702.

The online version of this article contains a data supplement.

The publication costs of this article were defrayed in part by page charge payment. Therefore, and solely to indicate this fact, this article is hereby marked "advertisement" in accordance with 18 USC section 1734.

were conducted in agreement with the Helsinki Declaration of 1975, revised in 1983.

Antibodies, reagents, and Western blotting

The anti-CD20 mAb rituximab was kindly provided by Roche Nederland BV (Woerden, The Netherlands), the anti-CD20 mAb GA101 was provided by Roche Glycart (Schlieren, Switzerland), and the goat anti–human (GAH) Fc-γ fragment–specific Ab was obtained from Jackson Immunoresearch Europe.

The pan-caspase inhibitor Q-VD was purchased from R&D Systems and Z-VADfmk from Alexis Biochemicals. Fludarabine, chlorambucil, nutlin, bendamustine, concanamycin A (concA), bafilomycin A (bafA), cytochalasin D (cytoD), propidium iodide (PI), and N-acetylcysteine (NAC) were purchased from Sigma-Aldrich. The proteasome inhibitor bortezomib was obtained from Janssen-Cilag. MitoTracker Orange and LysoTracker Red were purchased from Molecular Probes. FITC-labeled annexin V was purchased from IQ Products. Anti-CD2 allophycocyanin (clone S5.2) and FITC-conjugated rabbit anti–active caspase-3 mAb (catalog #559341) were purchased from BD Biosciences.

Preparation of cell lysates and Western blotting were performed as described previously.[25] Blots were probed with rabbit anti–cleaved caspase-3 mAb (catalog #9664; Cell Signaling Technology), polyclonal rabbit anti–poly(adenosine diphosphate)-ribose polymerase (anti–PARP) Ab (catalog #9452; Cell Signaling Technology), or cathepsin B (AF953; R&D Systems) and antiserum to β-actin (Santa Cruz Biotechnology) or tubulin (Cell Signaling Technology).

Immunoreactive proteins were visualized using IRDye 680 donkey anti–rabbit IgG, IRDye 800 donkey anti–goat IgG, or IRDye 800 donkey anti–mouse IgG (Westburg) as secondary Abs. Blots were scanned on an Odyssey imager (LI-COR Biosciences).

MDW933 detection of active GBA in CLL cells

Glucocerebrosidase (GBA) from CLL cell extracts were labeled in vitro with green fluorescent MDW933.[26] The lysate (20 μg of total protein) was incubated for 30 minutes at 37°C with the probe dissolved in McIlvaine buffer (150mM citrate-Na_2HPO_4, pH 5.2, 0.2% [wt/vol] sodium taurocholate, and 0.1% [vol/vol] Triton X-100). After incubation, samples were resolved under standard conditions on 10% SDS-PAGE. The resulting gels were analyzed by fluorescence scanning on a Typhoon Variable Mode Imager (Amersham Biosciences), 600 PMT, medium sensitivity, 200-μm pixel size, MDW933 (488 λem, 520bp40 λex).

In vitro stimulation of CLL cells

PBMCs from CLL patients (> 90% $CD5^+CD19^+$ cells) were stimulated with CD40 ligand (CD40L) transfected NIH3T3 (3T40L) cells as described previously.[4] Briefly, 5×10^6 CLL cells/well were added to 6-well plates coated with irradiated (30 Gy), CD40L-transfected NIH3T3 cells. Nontransfected 3T3 cells were used as negative controls. After 3 days, CLL cells were gently removed from the fibroblast layer and used in further experiments. In analogous experiments, CLL cells were cocultured with autologous T cells activated with 1 μg/mL of anti-CD3 (clone 1XE; Sanquin) and 5 μg/mL of anti-CD28 (clone 15E8; Sanquin) or soluble anti-CD40 (clone 14G7; Sanquin). After 3 days, cells were used in further experiments.

Induction and analysis of apoptosis and caspase-3 activation

For apoptosis induction, 3T3- or 3T40L-stimulated CLL cells (at a concentration of 1.5×10^6/mL) were incubated with the indicated anti-CD20 mAbs (10 μg/mL) for 24 hours. Cross-linking GAH Ab (indicated as XL) (50 μg/mL) was added 30 minutes after the CD20 mAbs. In combination experiments, cells were incubated with GA101 and cytotoxic drugs for 48 hours. Fludarabine was used at a final concentration of 25 and 50μM, bortezomib at 15 and 30nM, nutlin at 5 and 10μM, chlorambucil at 5 and 10μM, and bendamustine at 50 and 100μM.

The pan-caspase inhibitors Q-VD or Z-VAD-FMK and the ROS scavenger NAC were added 30 minutes before and cytoD, concA, or bafA 45 minutes before the indicated mAbs.

Apoptosis was analyzed by evaluation of mitochondrial membrane potential with MitoTracker Orange (Molecular Probes) according to the manufacturer's recommendations or by annexin V/PI staining, as described previously.[27] The percentage of apoptotic cells was calculated as follows: 100% − annexin V^-/PI^- (viable) cells. In some experiments, data are expressed as specific cell death (because of heterogeneous levels of basal apoptosis), which was defined as: percentage of cell death in stimulated cells − percentage of cell death in medium control.

For analysis of active caspase-3, cells were fixed and permeabilized (eBioscience) and then stained with FITC-conjugated rabbit anti–active caspase-3 mAb (BD Biosciences).

Samples were analyzed on the FACSCalibur flow cytometer (BD Biosciences) and CellQuest Version 4.0 software (BD Biosciences) was used for data acquisition. Data were analyzed with FlowJo Version 7.6 software (TreeStar).

DNA fragmentation was analyzed using flow cytometry after PI labeling of apoptotic nuclei as described previously.[28] In brief, after apoptosis induction (as described in "Induction and analysis of apoptosis and caspase-3 activation"), cells were put on ice and then centrifuged. While vortexing, cells were resuspended in 200 μL of hypotonic solution containing 25 μg/mL of PI, 100 μg/mL of RNAse, and 0.1% Triton X-100 in 0.1% Na-citrate solution. Cells were incubated on ice for 1 hour in the dark and analyzed by flow cytometry. The sub-G_1 peak represents apoptotic cells.

Light and confocal microscopy

Homotypic aggregation (HA) was assessed with light microscopy. Cells were incubated with the indicated anti-CD20 mAbs in flat-bottomed, 48 well-plates, and 24 hours later were viewed with a Leica DCF 320 inverted microscope using 10× or 20× maagnification. Images were acquired using a Leica DMIL camera type 090-135.002 and were processed with Leica Application Suite Version 3.4 software.

For confocal microscopy, after incubation with GA101 at different time points, cells were incubated with 25nM LysoTracker Red for 15 minute, washed with cold PBS, and then fixed with 2% paraformaldehyde on ice for 5 minutes. After fixation, cells were seeded onto glass object slides for confocal analysis using a Leica TCS SP2 confocal system equipped with an Ar/Kr laser with a 63× objective, and images were taken in glow-over-under mode.

Lysosomal volume measurement

To assess lysosomal volume, after incubation with GA101, cells were labeled with 25nM LysoTracker Red at different time points. FL-2 fluorescence of LysoTracker-labeled cells was measured on a FACSCalibur flow cytometer (BD Biosciences) 1 hour after labeling. Unlabeled cells were used as a background control. The number of lysosomes per cell was determined by 2 independent investigators blinded to which cells they were observing.

Assessment synergistic or additive effects of GA101 with cytotoxic drugs and statistics

To assess possible synergistic or additive effects, drug interactions were analyzed as described previously.[29,30] In short, observed survival corrected for baseline apoptosis of the sample is plotted against expected survival, calculated from the fraction of surviving cells of samples treated with the individual drugs and GA101 (expected survival = survival drug × survival GA101).

The diagonal line (XY line) represents the situation when the observed survival was equal to the predicted survival. Dots beneath this line indicate synergistic interactions (observed survival < expected survival). Dots above the XY line represent additive interactions (observed survival > expected survival, but < survival of the most active single drug).

The Shapiro-Wilk normality test was performed to test Gaussian distribution. When there was Gaussian distribution, a 2-sided paired *t* test was used to analyze differences between the groups. The 2-tailed Mann-Whitney *U* test was used to analyze differences between 2 groups, and a Wilcoxon matched-pairs test was used to analyze differences between paired samples when there was no Gaussian distribution. $P < .05$ was considered statistically significant.

Table 1. Patient characteristics

ID no.	Sex	Age, y	IgHV	Genetic aberration	p53	Rai stage	Previous therapy
1	F	49	Mut	del13q14	Functional	1	None
2	F	64	Mut	None	Functional	2	ClbP
3	M	59	Mut	None	Functional	3	None
4	M	64	UM	del13q14, del5q15	Functional	1	None
5	F	44	Mut	del13q14	Functional	2	Clb
6	M	75	Mut	del11q22	Functional	1	None
7	M	64	Mut	del13q14, del5q15, t(14q32)	Functional	3	Clb
8	F	75	Mut	None	Functional	4	None
9	M	65	Mut	del13q14, t(14q32)	Functional	4	Clb
10	M	60	UM	trisomie 12	ND	0	Clb
11	M	51	UM	trisomie 12	Functional	1	Clb
12	M	77	UM	del13q14, del11q22, del17p13	Functional	2	ClbP
13	M	74	UM	None	Functional	2	None
14	F	89	Mut	None	Functional	0	None
15	M	59	Mut	del13q14, del11q22	Functional	2	Clb, F
16	F	82	Mut	None	Functional	1	None
17	M	77	Mut	del11q22	Functional	2	None
18	F	85	Mut	None	ND	1	None
19	F	62	Mut	ND	ND	1	None
20	M	59	Mut	None	Functional	3	None
21	M	51	UM	trisomie 12	Functional	1	Clb
22	M	44	UM	None	Functional	2	None
23	M	66	UM	ND	ND	0	None
24	M	59	UM	ND	Functional	0	None
25	M	60	UM	del11q22	Functional	2	Clb, Ofa, FCR + P
26	F	59	UM	del17p13 67%, t(14q32)	Nonfunctional	1	None
27	M	83	Mut	del17p13 53%, del13q14	Nonfunctional	4	Clb
28	M	54	Mut	ND	Nonfunctional	1	None
29	V	63	Mut	del13q14	Functional	ND	ND
30	M	58	Mut	ND	Functional	3	ND
31	M	59	Mut	ND	Functional	3	ND
32	M	63	Mut	del13q14, del14q32	Functional	3	ND

Mut indicates mutated IgHV genes; UM, unmutated IgHV genes; Clb, chlorambucil; ClbP, chlorambucil + prednisone; F, fludarabine; FCR, fludarabine, cyclophosphamide, rituximab; Ofa, ofatumumab; P, prednisone; and ND, not determined.

Results

CD40 stimulation sensitizes CLL cells to GA101-induced cell death

The induction of cell death by GA101[15] and GA101 and cross-linker (GXL) was compared with rituximab plus cross-linker (RXL) in CD40-stimulated (3T40L) CLL cells and unstimulated (3T3) CLL cells of 13 patients. Patient characteristics are listed in Table 1 (patients 1-13). CD40 stimulation induces resistance to various conventional drugs[3] such as roscovitine, a cyclin-dependent kinase inhibitor that acts via the Mcl-1/Noxa axis and induces classic caspase dependent apoptosis.[3,31] In contrast, CD40 stimulation sensitized to anti-CD20–mediated cell death (Figure 1A) triggered via RXL or GA101, with a maximum at 24 hours at a concentration of 10 μg/mL (data not shown). CLL cells with unmutated and mutated Ig variable heavy genes (IGHV) had similar sensitivity to anti-CD20–mediated death (Figure 1A top panels). GA101 induced cell death in the absence of a secondary cross-linking mAb, in contrast to rituximab (Figure 1A bottom panel). GXL increased cell death of control 3T3 and CD40-stimulated CLL cells, whereas XL alone did not induce cell death. Representative annexin V/PI plots are shown in Figure 1B. Assessment of cell death by evaluation of mitochondrial membrane potential with MitoTracker gave equivalent results as obtained with annexin V/PI staining (Figure 1C). Furthermore, the induction of a sub-G_1 peak as a result of DNA fragmentation was observed 24 hours after incubation with RXL, G, and GXL (Figure 1D). To investigate the kinetics of CD40-induced sensitization to anti-C20 mAbs, cells were stimulated with CD40L for different time points (6, 24, and 48 hours) and then incubated with anti-CD20 mAbs. CD40-induced sensitization to GA101-induced cell death was optimal after 48 hours of stimulation with CD40L (Figure 1E). CD40-induced sensitization to GA101 occurred with similar timing as CD40-induced resistance to cytostatic drugs (Figure 1E). Stimulation with CD40L for 72 hours did not further increase sensitivity to CD20 mAbs or drug resistance (data not shown).

A purported source of the CD40L in vivo are T cells residing in the lymph nodes.[1,3-5,7,8] Therefore, we investigated whether autologous T cells could provide sufficient CD40 stimulation to enhance GA101-induced cell death. CLL cells were cocultured with autologous T cells using the endogenous ratios of CLL versus T cells present in the PBMC fraction. T cells were activated for 3 days via combined anti-CD3/CD28 mAbs, which induces expression of CD40L (supplemental Figure 3, available on the *Blood* Web site; see the Supplemental Materials link at the top of the online article), and then the CLL cells were tested for sensitivity to CD20-mediated cell death. Activated T cells were able to significantly increase sensitivity to RXL- and GA101-induced cell death (Figure 1F). The sensitivity toward roscovitine was not affected using activated T cells in this particular setup, showing that the types of cell death induced by CD20 stimulation or drugs are distinct. The relatively weak stimulus of soluble anti-CD40 (Figure 1F) caused only a slight increase in RXL-induced cell

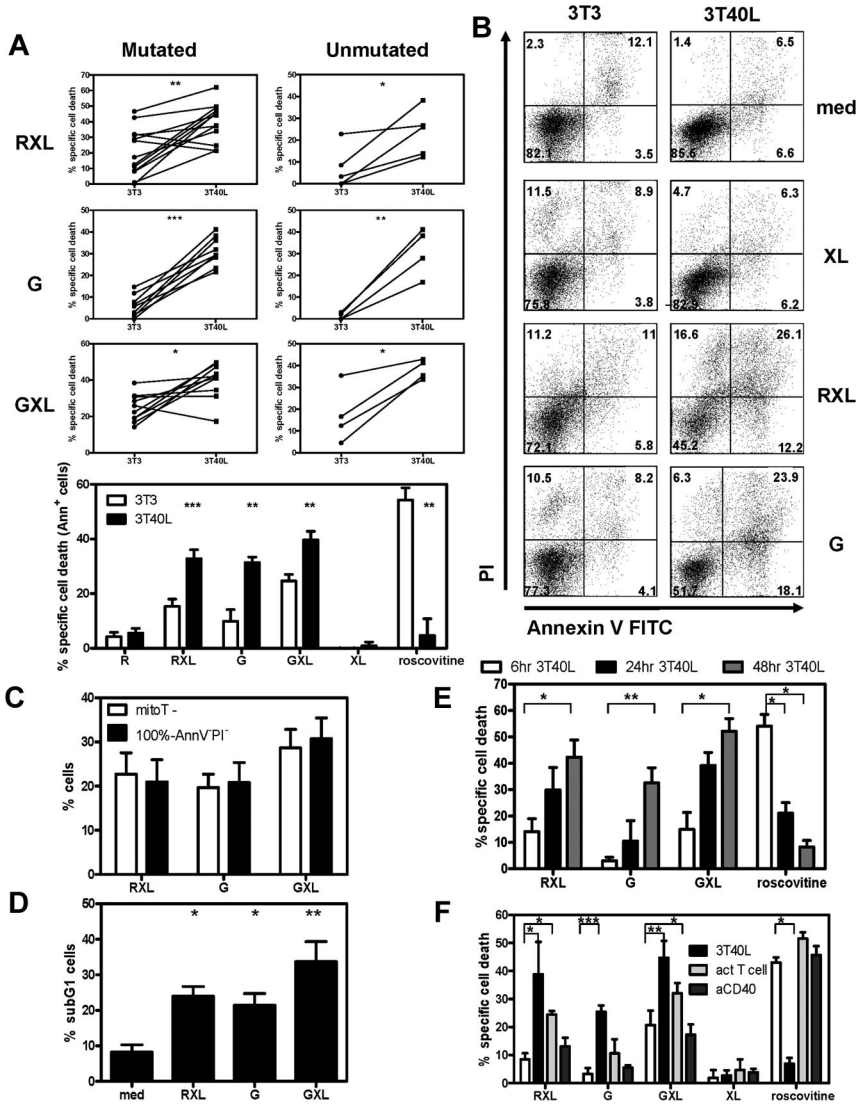

Figure 1. CD40 stimulation induces drug resistance but sensitizes CLL cells to GA101-induced cell death. (A) PBMCs from CLL patients were cultured on 3T3 murine fibroblasts or 3T3-expressing human CD40L as described in "Methods." After 3 days, 3T40L and 3T3 CLL cells were removed from the fibroblast layer and incubated with the indicated anti-CD20 mAbs. R indicates rituximab; G, GA101. Where indicated, cross-linking (XL) GAH Ab (50 μg/mL) was added 30 minutes after the anti-CD20 mAbs RXL and GXL. After 24 hours, apoptosis was analyzed by measuring phosphatidyl serine (PS) and annexin V exposure by flow cytometry. Top: results from individual patients (mutated: mutated IgHV genes, unmutated: unmutated IgHV genes) Bottom: averaged results from 13 CLL patients (8 mutated and 5 unmutated). Data are presented as the percentage of specific cell death, in which the background apoptosis in the absence of reagents was subtracted from the observed values in each incubation (mean ± SEM). $^{**}.001 < P < .01$ and $^{***}P < .001$ significant difference from control (3T3). (B) Representative annexin V/PI FACS plots from 3T3 and 3T40L CLL cells incubated for 24 hours with XL alone, RXL and G, respectively. (C) CD40-stimulated CLL cells were incubated for 24 hours with RXL, G, and GXL, and cell death was analyzed in parallel by annexin V/PI or MitoTracker FACS staining. Stainings gave similar results in percentage of dead cells. Averaged results from 3 independent experiments (n = 7 patients; mean ± SEM). Black bars indicate dead cells as analyzed by annexin V/PI staining (% dead cells = 100% − annexin V^-PI^- cells). (D) Percentage of sub-G_1 cells in CD40-stimulated CLL cells 24 hours after incubation with RXL, G, and GXL. Averaged results from 5 CLL patients are presented as the percentage of sub-G_1 cells (mean ± SEM). $^{*}.01 < P < .05$ and $^{**}.001 < P < .01$ significant difference from control (medium). (E) Time course of CD40 stimulation (6, 24, and 48 hours) and subsequent incubation with RXL, G, GXL, and roscovitine. After 24 hours, apoptosis was analyzed by measuring MitoTracker signal by flow cytometry. Averaged results from 7 CLL patients are presented as percentage specific cell death (mean ± SEM). $^{*}.01 < P < .05$; $^{**}.001 < P < .01$. (F) CLL cells stimulated for 72 hours with 3T3, 3T40L, and CD3/CD28 activated autologous T cells (act T cell) or with soluble anti-CD40 (aCD40) were incubated with RXL, G, GXL, and roscovitine. After 24 hours, apoptosis of CLL cells was analyzed by measuring MitoTracker signal in $CD2^-$ cells by flow cytometry. Averaged results from 3 CLL patients are presented as percentage specific cell death. $^{*}.01 < P < .05$; $^{**}P < .001$.

death. Therefore, CD40 stimulation of CLL cells via a coculture system or via endogenous activated T cells sensitized to CD20-mediated cell death. In subsequent experiments, GA101 was tested in the absence of a cross-linking mAb, except where indicated.

GA101 induces cell death in CD40-stimulated CLL cells in a nonapoptotic manner

After incubation with GA101, CD40-stimulated CLL cells showed processing of the effector caspase-3 as determined by FACS analysis (Figure 2A). Regarding the amount of caspase 3 activation, 3 categories of cells could be discerned: low, intermediately, and highly positive cells (indicated in Figure 2A). Cells treated with GA101 showed increases in the intermediate category, whereas the positive control for full caspase-3 processing (roscovitine) displayed high staining. PARP is a substrate of caspase-3 and PARP cleavage is a hallmark in classic caspase-dependent apoptosis.[32] Basal levels of cleaved caspase-3 and PARP were already observed on Western blot analysis in CD40-stimulated CLL cells and GA101 induced no further increase (Figure 2B). As a positive control, cells were treated with roscovitine. As expected, PARP cleavage and caspase-3 activation by roscovitine were blocked in the presence of 20μM Q-VD (Figure 2B). In contrast, there was no clear correlation among the amount of caspase-3 activation, PARP cleavage, and the percentage of dead cells found for GA101. Moreover, although GA101 induced caspase-3 activation (as measured by intracellular staining), cell death was not blocked in the presence of Q-VD (20μM) or Z-VAD (100μM; Figure 2C). In addition, using an alternative measure of viability (the MTS assay) for CD40-stimulated CLL cells treated with anti-CD20 mAbs showed only a partial decrease, whereas control CLL cells treated with roscovitine displayed a clear reduction in metabolic activity (data not shown). Finally, CD40 stimulation of CLL cells generally does not trigger proliferation either alone[33] or in combination with anti-CD20 mAbs. Therefore, cell death by GA101 occurred via a nonclassic and/or caspase-independent mechanism.

GA101 induces actin polymerization–dependent homotypic aggregation and cell death in CD40-stimulated CLL cells

Recent studies have shown that type II anti-CD20 mAbs induced strong HA and subsequent cell death in Raji cells and primary CLL cells.[21,22] HA requires active reorganization of the cytoskeleton. It

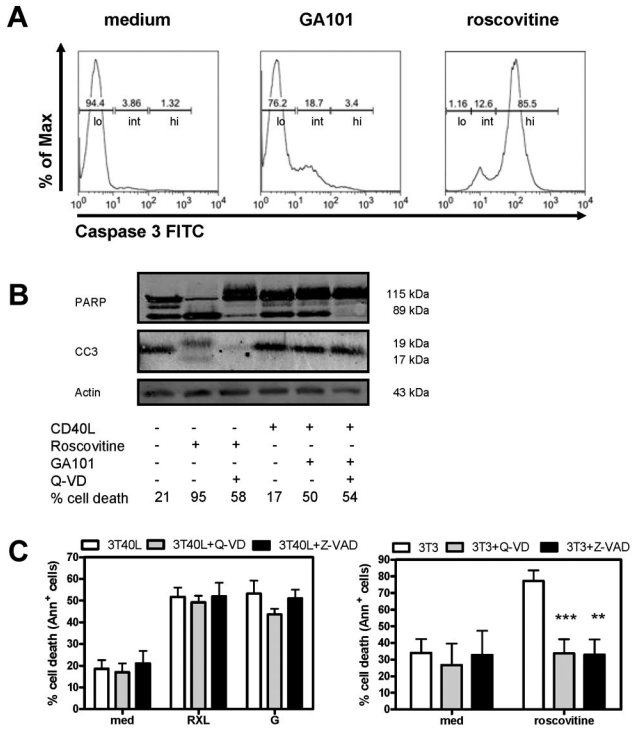

Figure 2. GA101 induces nonapoptotic cell death in CD40-stimulated CLL cells. (A) Representative FACS plots of intracellular active caspase-3 staining of CD40-stimulated CLL cells incubated with GA101 for 24 hours. As a positive control, unstimulated CLL cells incubated with roscovitine are shown. Indicated are low (lo), intermediately (int), and highly (hi) caspase-3 positive cells. (B) Western blot for cleaved PARP and active caspase-3 of cell lysates from CD40-stimulated CLL cells incubated with GA101 for 24 hours. As a positive control, unstimulated CLL cells treated with roscovitine are shown. Cleaved caspase 3 (CC3; 19 and 17 kDa) and caspase-3–induced cleavage fragment of PARP-1 of 89 kDa in the presence or absence of 20μM of Q-VD are shown. Percentage cell death as assessed with MitoTracker is indicated. Results are representative of 4 experiments. (C) RXL- and GA101-induced cell death in CD40-stimulated CLL cells was not blocked by 100μM Z-VAD or 20μM Q-VD (left). Right: roscovitine-induced cell death in unstimulated CLL cells was blocked by Z-VAD or Q-VD (positive control). Data are presented as percentage specific cell death (mean $\pm$ SEM from 4 independent experiments). **.001 $< P <$ .01 and ***$P <$ .001 significant difference from controls (3T3).

has been shown previously that CD40 stimulation induces homotypic adhesion in normal B cells,[34] although this was not confirmed for CLL cells.[35] Figure 3 shows mild HA of CLL cells after CD40 stimulation, which was strongly increased by GA101 or GXL. To determine whether the processes of HA and cell death were functionally linked, cells were treated with cytoD, an agent that inhibits actin polymerization. CytoD completely blocked GA101 and RXL induced HA (Figure 3) and cell death in CD40-stimulated CLL cells (Figure 4A), suggesting a clear dependence on actin reorganization.

CD40 stimulation sensitizes CLL cells to GA101-induced cell death via a lysosome-dependent mechanism

Our data suggested nonapoptotic cell death of CD40-stimulated CLL cells by GA101. Lysosomal membrane permeabilization (LMP) and subsequent lysosomal cell death resulting from the release of hydrolases into the cytosol is one proposed cell death mechanism induced by type II anti-CD20 mAbs.[21,22] To determine the involvement of lysosomes, CD40-stimulated CLL cells were pretreated with concA or bafA, both agents that inhibit the acidification of lysosomes by blocking V-ATPases.[36] HA was not blocked in the presence of concA (Figure 3), but GA101-induced cell death was completely blocked in cells pretreated with concA or bafA (Figure 4A). This suggested that the process of HA itself is lysosome independent, but that the subsequent cell death is lysosome dependent. Lysosomal swelling, LMP, and burst are characteristics of lysosomal cell death.[37] Lysosomal volume of cells incubated with GA101 at different time points was assessed using LysoTracker. FACS analysis of CD40-stimulated CLL cells after 2 hours of incubation with GA101 showed a peak in LysoTracker signal (Figure 4B), followed by a decrease after 4-6 hours, suggesting an initial increase in volume or numbers of lysosomes after 2 hours, followed by LMP and burst after 4-6 hours. This pattern was also reflected by the percentage of dead cells (data not shown), which increased after 4 hours. Furthermore, loss of LysoTracker signal coincided with loss of mitochondrial membrane permeability (data not shown), indicating that the process of lysosomal rupture and cell death are correlated.

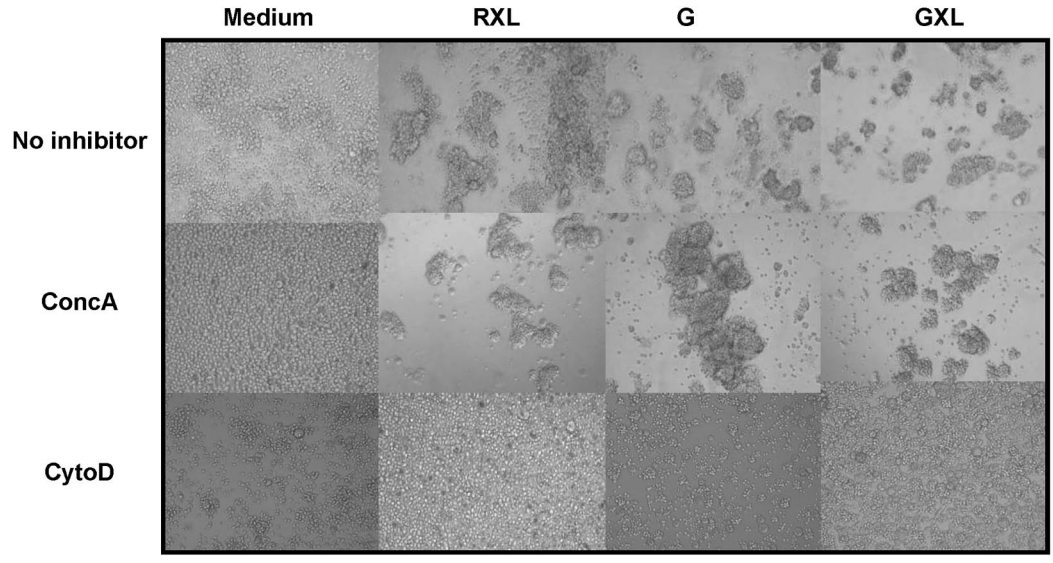

Figure 3. GA101 induces actin polymerization–dependent HA and cell death in CD40-stimulated CLL cells. 3T40L CLL cells were incubated with RXL, G, or GXL, respectively. Cells were preincubated with 100nM concA or 1μM cytoD for 45 minutes before the addition of anti-CD20 mAbs. After 24 hours, HA was assessed by light microscopy. Original magnification, 20$\times$. Data are representative of 10 experiments.

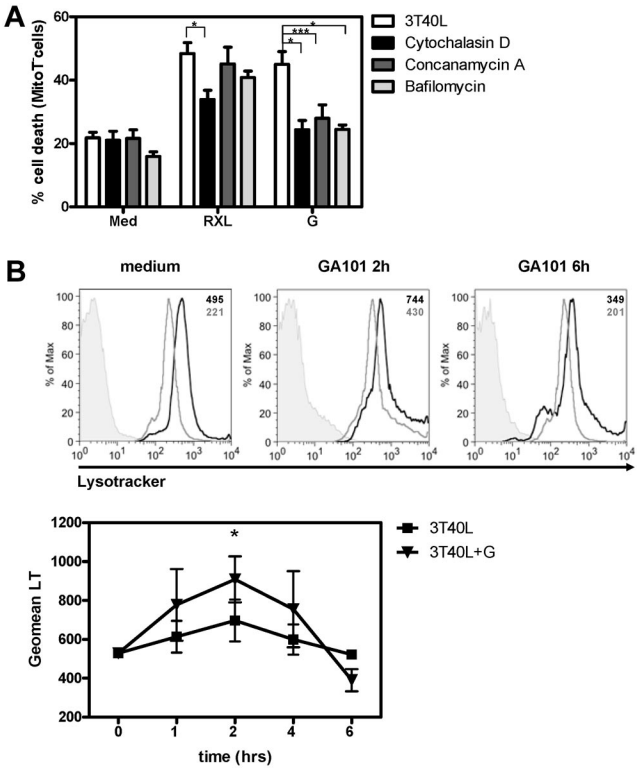

Figure 4. GA101 induces lysosomal swelling and burst and cell death is blocked by cytoD and concA. (A) Before incubation with RXL, G, or GXL, 3T40L CLL cells were pretreated with 1μM cytoD, 100nM concA, or 200nM bafA. After 24 hours, cell death was analyzed by measuring MitoTracker signal by flow cytometry. Averaged results from 8 CLL patients are presented as percentage cell death (mean ± SEM). (B) Top: Histograms showing LysoTracker signal in CD40-stimulated CLL cells in medium after 2 and 6 hours of incubation with GA101 in the presence (light gray line) and absence (black line) of concA. Unstained control is shown in shaded gray. In the right upper corner the individual Geomean of LysoTracker (LT) of every sample is shown. Bottom: After 1, 2, 4, and 6 hours of incubation with GA101, CD40-stimulated CLL cells were labeled with LysoTracker and the signal was analyzed by flow cytometry. *$.01 < P < .05$; ***$P < .001$.

LysoTracker-labeled cells incubated with GA101 were visualized by confocal microscopy. As a result of HA, large clusters of cells were observed after incubation with GA101 (Figure 5A arrow), and the distribution of lysosomes in individual cells was studied. Strikingly, the distribution and amount of lysosomes were very different between CD40-stimulated and -unstimulated CLL cells (Figure 5A-B). CD40-stimulated CLL cells showed increased numbers of bright LysoTracker-positive lysosomes, whereas unstimulated CLL cells contained only a small amount of lysosomes in the perinuclear region (Figure 5A medium control). In addition, the mean fluorescence intensity of LysoTracker signal in CD40-stimulated cells (3T40L) was 4 times higher than in unstimulated CLL cells (3T3; Figure 5B). After 2 hours of incubation with GA101, CD40-stimulated CLL cells showed both a further increase in LysoTracker signal and a relocalization of lysosomes around the nucleus, which disappeared after 4 hours of incubation (Figure 5A), thereby confirming the FACS data (Figure 4B). Importantly, the GA101-induced increase in lysosomal numbers and/or volume and activity was not observed in unstimulated (3T3) CLL cells (Figure 5A). Quantification of the number of lysosomes per cell showed that CD40 stimulation significantly increased the number of lysosomes per cell (Figure 5B right). GA101 treatment increased the number of lysosomes further (2 hours), whereas a decrease in lysosomal number was observed after 6 hours of incubation with GA101, suggesting a lysosomal burst. To confirm the observed increase in lysosomal content in CLL cells (patients 29-32 in Table 1) after CD40 stimulation, levels of the lysosomal hydrolases cathepsin B and active glucocerebrosidase (GBA), were measured by Western blot and by in vitro labeling of active GBA with the recently developed compound MDW933,[26] respectively. Clearly, an increase in both hydrolases was observed after CD40 stimulation (Figure 5C). These data suggest that by increasing the number and activity of lysosomes in the cell, CD40 stimulation sensitizes CLL cells to lysosomal cell death by GA101. This was confirmed by highest LysoTracker signal after 48 hours of CD40 stimulation (Figure 5D), the time point at which sensitization to anti-CD20 mAbs is at a maximum level (Figure 1E).

Recently, we described that cross-linking of Rituximab (RXL) induces ROS dependent cell death in CD40-stimulated CLL cells.[23] Of note, whereas the ROS scavenger NAC significantly inhibited RXL-induced cell death (Figure 5E), no inhibition was observed in GA101-induced cell death in the presence of NAC (Figure 5E), making a role for ROS in GA101-induced cell death less likely. An important question is whether lysosomes are involved in RXL-induced cell death of CD40 stimulated CLL cells. RXL-induced cell death was not blocked in the presence of concA (Figure 4A). Moreover, Figure 5F shows that in contrast to GA101, RXL induces no increase in LysoTracker signal or relocalization of lysosomes. These data suggest that RXL and GA101 induce cell death in CD40-stimulated CLL cells via a different mechanism.

Finally, the effect of Q-VD, cytoD, and concA on GA101-induced increase in LysoTracker signal in CD40-stimulated CLL cells was tested (Figure 5G). In line with previous results, Q-VD did not block HA or increase in LysoTracker signal (Figure 5G). Interestingly, cytoD blocked HA but did not block the increase in LysoTracker signal. As expected, concA did not block HA, but blocked the increase in LysoTracker signal (Figure 5G).

Additive cell death induction in drug resistant CLL cells by combination treatment of GA101 and cytotoxic drugs

Next, we tested the effect of a combination treatment of GA101 with cytotoxic drugs in CD40-stimulated CLL cells with mutated (n = 7) and unmutated (n = 5) IGHV genes and p53 dysfunctional CLL cells (n = 3). Patient characteristics are listed in Table 1 (patients 14-28). The p53-independent proteasome inhibitor bortezomib (15 and 30nM) and the following cytotoxic drugs with a p53-dependent mode of action were tested in combination with GA101: bendamustine (50 and 100μM), chlorambucil (5 and 10μM), fludarabine (25 and 50μM), and nutlin (5 and 10μM). Bendamustine is a mechlorethamine derivative with alkylating and purine-analog–like activity. Chlorambucil is a nitrogen mustard alkylating agent that induces a p53 response after induction of DNA damage.[38] Fludarabine is a purine analog and triggers apoptosis via a p53 response that induces the expression of Puma.[25,39] Nutlins are the first highly selective small-molecule inhibitors of the p53-MDM2 interaction and are able to induce p53 irrespective of upstream signaling defects.[40] Nutlin-3a has shown promising cytotoxic activity against CLL.[41]

The sensitivity of unstimulated CLL cells to the different cytotoxic drugs was tested, and there was no difference in sensitivity between CLL cells with mutated and unmutated IGHV genes (supplemental Figure 1). As expected, p53-dysfunctional CLL cells showed resistance to the p53-dependent drugs chlorambucil, fludarabine, and nutlin and partial resistance to bendamustine. However, these cells were sensitive to bortezomib, which acts via a p53-independent mechanism[42] (supplemental Figure 1).

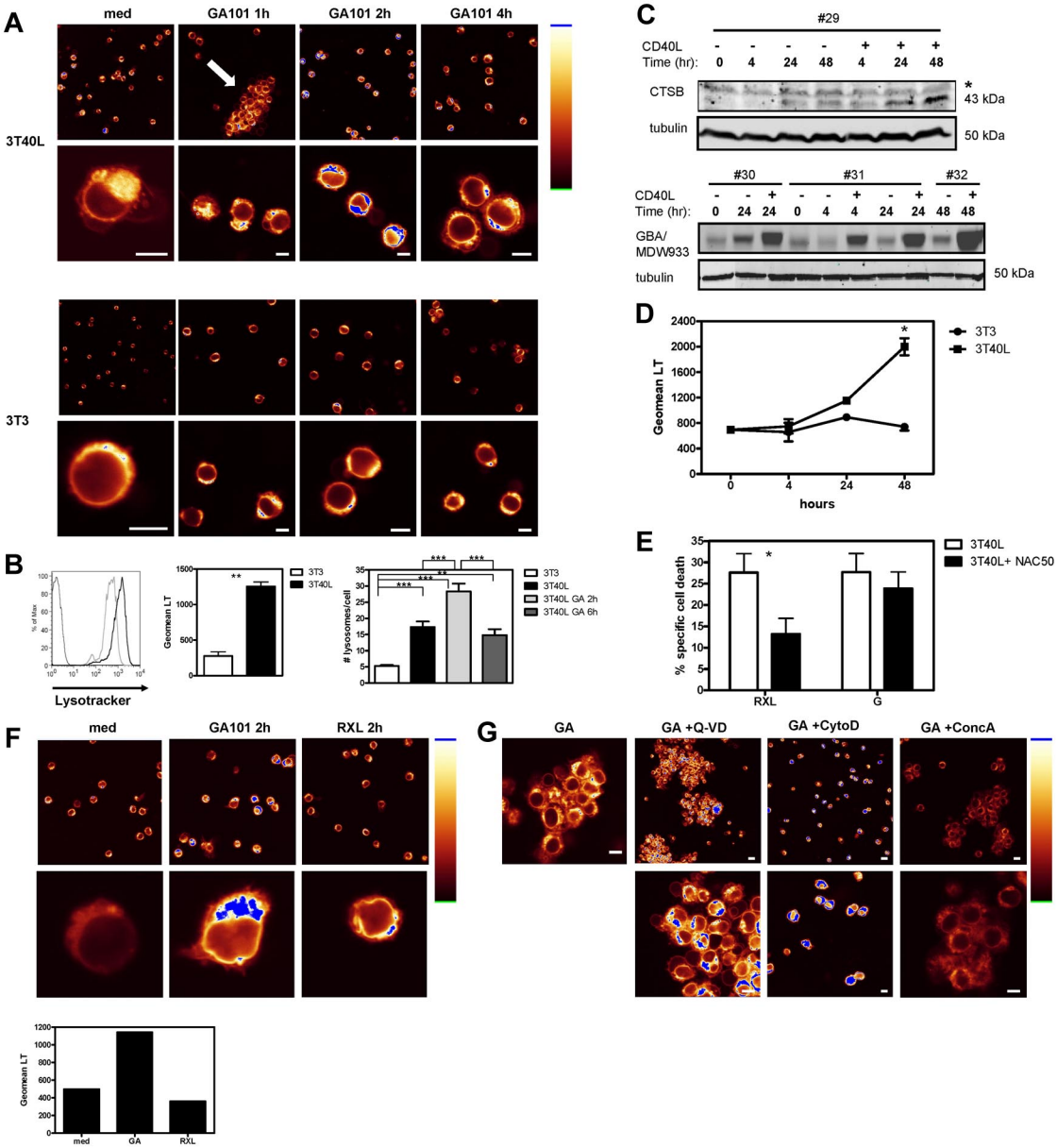

Figure 5. CD40 stimulation sensitizes CLL cells to GA101-induced cell death via a lysosome-dependent mechanism. (A) Confocal microscopy of LysoTracker-labeled unstimulated (bottom panel) and CD40-stimulated CLL cells (top panel) after different time points of treatment with GA101. Shown is the distribution of lysosomes in individual cells visualized in glow-over-under (right: glow-over-under color scale with the highest intensity in blue). Note the increase in both number and activity of lysosomes in CD40-stimulated CLL cells (3T40L medium) compared with unstimulated cells (3T3 medium). After 1 hour of incubation with GA101, CD40-stimulated CLL cells showed clustering of cells (arrow). After 2 hours of incubation with GA101, an increase in LysoTracker signal (blue) was observed in CD40-stimulated CLL cells (top panel), whereas no increase was observed in unstimulated CLL cells. Data shown are representative of 3 individual experiments, each with $>$ 100 cells and identical settings for imaging. Scale bar indicates 5 μm. (B) CD40-stimulated and unstimulated CLL cells were labeled with LysoTracker and analyzed by flow cytometry. Left: representative FACS plot of LysoTracker signal in unstimulated (gray line) and CD40-stimulated CLL cells (black line). Thin black line: unstained control. Middle mean fluorescence intensity (MFI) of LysoTracker in unstimulated and CD40-stimulated CLL cells. Averaged results from 5 CLL patients (mean ± SEM) ***.001 $<$ P $<$ .01 significant difference from control (3T3). Right: Quantification of the number of lysosomes per cell in 3T3, 3T40L, 3T40L + GA 2-hour and 3T40L + GA 6-hour–stimulated CLL cells. Averaged results from 2 independent observers (mean ± SEM) **.001 $<$ P $<$ .01; ***P $<$ .001. (C) Top: Representative Western blot of the 43-kDa procathepsin B (CTSB) of cell lysates from 3T3 and 3T40L CLL cells for 4, 24, or 48 hours. The asterisk (*) marks the position of an aspecific protein band reacting with the antiserum. Tubulin was used as loading control on the same gel. Blot is representative of 4 mutated patients tested. Contrast and brightness were adjusted for optimization. Bottom: in vitro labeling of active GBA in unstimulated and CD40-stimulated CLL cells for different time points (3 different patients). Tubulin was used as loading control on the same samples, run in parallel on a standard SDS-PAGE gel and followed by Western blot. (D) CLL cells were stimulated with 3T3 or 3T40L in a time course (4, 24, and 48 hours), after which time LysoTracker signal was analyzed by flow cytometry. Averaged results from 3 CLL patients are presented as Geomean of LysoTracker signal (mean ± SEM) *.01 $<$ P $<$ .05. (E) CD40-stimulated CLL cells were incubated with RXL or GA101 in the presence or absence of NAC. After 24 hours, cell death was analyzed by measuring MitoTracker signal by flow cytometry. NAC significantly blocked RXL-induced cell death of CD40-stimulated CLL cells, but not GA101-induced cell death. Data are presented as percentage specific cell death (mean ± SEM). Averaged results from 10 independent experiments are shown. *.01 $<$ P $<$ .05. (F) Confocal microscopy of LysoTracker-labeled, CD40-stimulated CLL cells after 2 hours of treatment with GA101 or RXL. Shown is the distribution of lysosomes in individual cells visualized in glow-over-under. GA101 induces an increase in number and activity of lysosomes in contrast to RXL. Scale bar indicates 5 μm. Bar graph shows LysoTracker signal analyzed by flow cytometry. (G) Confocal microscopy of LysoTracker-labeled, CD40-stimulated CLL cells after 2 hours of treatment with GA101 (GA) in the presence or absence of Q-VD, cytoD, or concA. Note that HA and increase in LysoTracker signal were not blocked by Q-VD. An increase in LysoTracker signal was observed in the presence of cytoD, despite the absence of HA. ConcA blocked the GA101-induced increase in LysoTracker signal, but not HA. Scale bar indicates 5 μm.

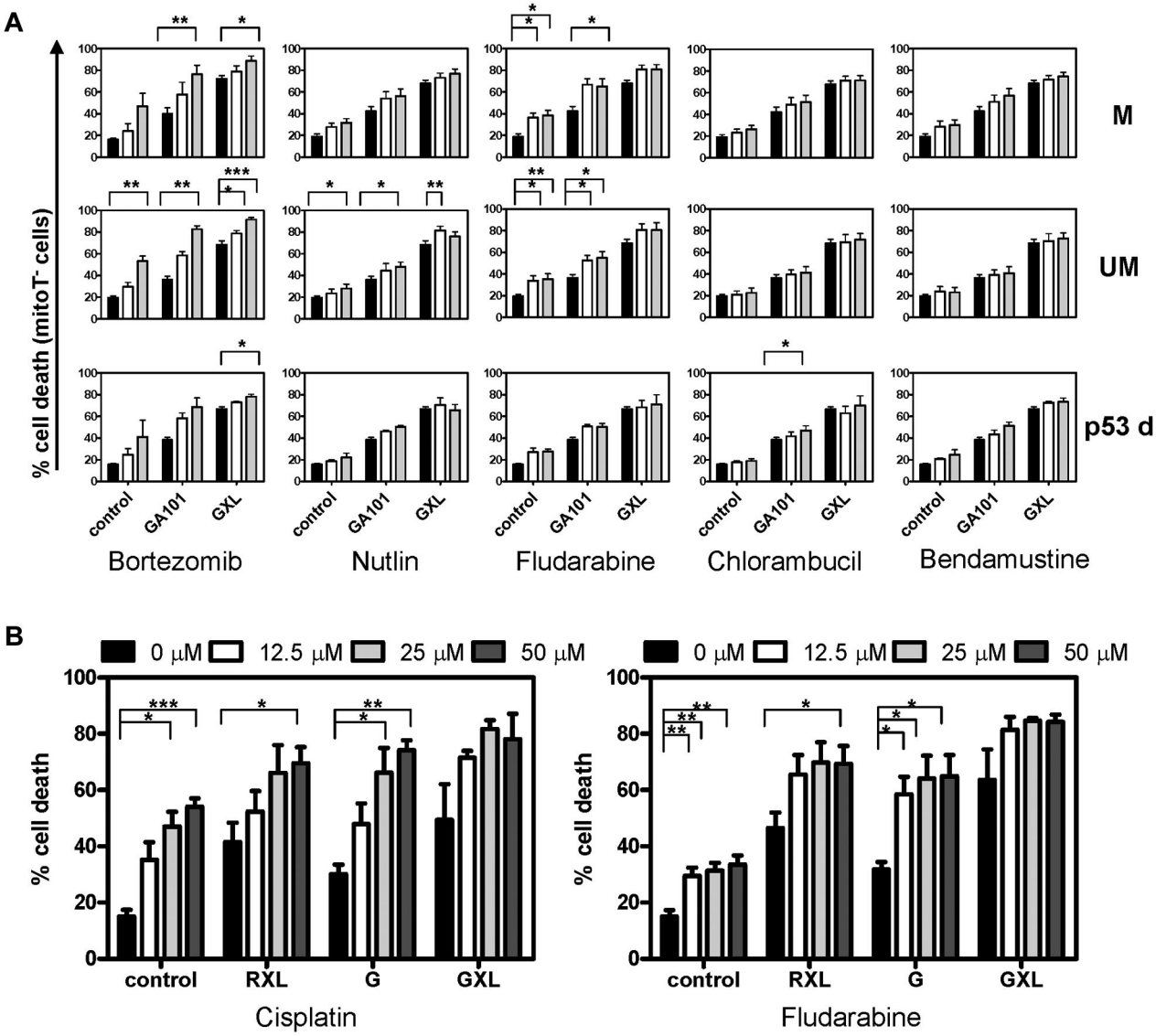

Figure 6. Cell death induction in drug-resistant CLL cells by the combination treatment of CD20 mAbs and cytotoxic drugs. (A) CD40-stimulated CLL cells were incubated with different concentrations of bortezomib, nutlin, fludarabine, chlorambucil, or bendamustine alone or in combination with GA101 or GXL. After 48 hours, cell death was analyzed by measuring MitoTracker signal by flow cytometry. Averaged results are presented as percentage cell death (mean ± SEM). *$.01 < P < .05$, **$.001 < P < .01$, and ***$P < .001$ significant difference compared with control. M indicates mutated IGHV genes (n = 7); UM, unmutated IGHV genes (n = 5); and p53d, p53-dysfunctional CLL cells (n = 3). Black bars indicate controls; white bars, low-concentration and gray bars, high-concentration cytotoxic drug (bortezomib 15 and 30nM; nutlin 5 and 10μM; fludarabine 25 and 50μM; chlorambucil 5 and 10μM; and bendamustine 50 and 100μM, respectively). (B) Averaged results from 4 CLL patients (3 with mutated and 1 with unmutated IGHV genes) treated with RXL, G, GXL, and fludarabine 12.5, 25, or 50μM or with RXL, G, and GXL and 12.5, 25, or 50μM cisplatin. After 48 hours, apoptosis was analyzed by MitoTracker staining by flow cytometry. Data are presented as percentage cell death (mean ± SEM). *$.01 < P < .05$, **$.001 < P < .01$, and ***$P < .001$ significant difference compared with control.

The results from the combination treatment of CD40-stimulated CLL cells with GA101 and cytotoxic drugs are shown in Figure 6A. As expected, CD40-stimulated CLL cells were fully or partially resistant to the cytotoxic drugs alone (left bars in each panel labeled "control"). However, cells were sensitive to GA101 and GXL, as shown in Figure 1. When combined with cytotoxic drugs, GA101 and especially GXL induced 80%-100% cell death in these drug resistant CLL cells. CD40-stimulated, p53-dysfunctional CLL cells were sensitive to GA101 and, in combination with cytotoxic drugs, apoptosis levels of 80% were observed (Figure 6A bottom panel; n = 3).

Synergistic or additive effects of GA101 and the cytotoxic drugs (assessed as described in "Methods") are shown in Table 2 and supplemental Figure 2. No significant synergistic effects were found.

High concentrations of chlorambucil and bendamustine showed statistically significant additive effects in CD40-stimulated CLL cells with mutated and unmutated IGHV genes. At 100μM, bendamustine also showed a significant additive effect in CD40-stimulated, p53-dysfunctional CLL cells. Nutlin induced significant additive effects in CLL cells with unmutated IGHV genes and in CD40-stimulated, p53-dysfunctional CLL cells (supplemental Figure 2); for 30nM bortezomib additive effects in CD40-stimulated, p53-dysfunctional CLL cells were observed. Fludarabine-containing regimens have been shown to be effective in CLL.[11] Furthermore, our recent studies showed synergistic effects of the ROS-inducing drug cisplatin and fludarabine regarding cell death induction of CLL,[43] and these drugs also enhanced cell death by RXL.[23] We therefore tested whether low concentrations of

Table 2. Synergistic or additive effects of GA101 and cytotoxic drugs

Mutation status/ treatment	Bortezomib	Nutlin	Fludarabine	Chlorambucil	Bendamustine
M					
GA	A	A	A	A*	A*
GXL	A	A	A	A*	A
UM					
GA	Syn	A*	A	A*	A***
GXL	Syn	A	A	A	A*
p53d					
GA	A	A**	A	A	A*
GXL	A*	A	A	A	A

Pooled results of 7 mutated (M), 5 unmutated (UM), and 3 p53-dysfunctional (p53d) patient samples treated with G or GXL in combination with different cytotoxic drugs.

A indicates additive trend; and Syn, synergistic trend; *$0.1 < P < .05$, **$.01 < P < .05$, and ***$P < .001$ for the statistically significant additive effect.

cisplatin or fludarabine in combination with GA101 induced cell death in drug-resistant CLL cells. Indeed, low concentrations of both cisplatin and fludarabine combined with RXL, but also G and GXL, induced strong cell death induction in CD40-stimulated CLL cells (Figure 6B).

Discussion

This study shows for the first time that cell death induced by the type II anti-CD20 mAb GA101 is enhanced in primary CD40-stimulated CLL cells. Our main finding was that by increasing lysosomal volume and number, CD40 stimulation sensitizes CLL cells to GA101-induced lysosomal cell death. These results extend those of recent studies showing type II–induced lysosomal cell death in cell lines,[21,22] and translate these findings into a physiologically relevant context. In contrast to the type I mAb rituximab, GA101 does not require a secondary cross-linking mAb to induce cell death in vitro. Finally, combination treatment of drug-resistant CD40-stimulated CLL cells with GA101 and cytotoxic drugs results in additive cell death induction, including in p53-dysfunctional CLL cells.

Although the contrasting effects of CD40-induced sensitization to anti-CD20 mAbs and CD40-induced drug resistance occur with similar kinetics, the underlying mechanisms are clearly different. First, CD40-induced sensitization to RXL is based on the formation of ROS,[23] whereas CD40-induced sensitization to GA101 is based on increased lysosomal number and volume (present results). Secondly, CD40-induced drug resistance is based on an increase in Bcl-2 family members and a decrease in BH3-only proteins, resulting in an antiapoptotic profile.[3,44] We and others have shown that Bcl-2 members and classic apoptosis involving activated caspase 3 do not play a role in anti-CD20–induced cell death.[21,23]

To translate the observation that CLL cells cultured on CD40L-expressing fibroblasts were more sensitive to anti-CD20 mAbs to a more physiologic setting, we also tested CLL cells cocultured with autologous CD3/CD28 activated T cells. The fraction of T cells in this setup is far less than that of the CLL cells, and the CD40 stimulation is likely to be less potent than in the coculture system, but enhanced sensitivity to anti-CD20 mAbs was still detectable. Using only soluble anti-CD40 mAbs did not significantly enhance sensitivity toward anti-CD20 mAbs, probably because of the rather weak CD40 signaling provided.[5] This could also be explained by different epitope binding and the absence of cross-linking in contrast to membrane-bound CD40L in 3T40L cells and activated T cells. Maximal resistance to chemotherapeutic drugs was only observed in CLL cells cocultured with 3T40L cells. There are several likely explanations for this. First, the mechanism of anti-CD20–induced cell death is clearly different from cell death induced by cytostatic drugs. The latter is classic mitochondrial apoptosis controlled by Bcl-2 members. In addition, induction of full drug resistance in CLL cells requires persistent CD40 and/or NF-κB signaling, resulting in strong up-regulation of Bcl-2 members Mcl-1, Bcl-XL, and Bfl-1.[3] In an experimental setting, such strong signaling can be provided by 3T40L cells, which express higher levels of CD40L than activated T cells (supplemental Figure 3).

As shown previously,[21] homotypic aggregation and cell death induced by GA101 were completely blocked by cytoD. Therefore, the process of HA seems to be essential for cell death induction, yet the exact mechanism behind GA101-induced HA remains to be determined. This is also not clear for other type II mAbs. GA101-induced HA was not dependent on ICAM-1 (data not shown). Increased sensitivity of CD40-stimulated CLL cells to GA101-induced cell death might be linked to increased HA as a result of CD40 stimulation.[34]

Lysosomal cell death has recently been determined to be an actual cell death mechanism rather than a downstream event of apoptotic cell death (for review, see Kroemer and Jaattela[37]). Decreased LysoTracker fluorescence may reflect LMP and/or an increase in lysosomal pH, meaning that this method is not absolutely specific for LMP.[45] However, these data, together with complete inhibition of cell death in the presence of concA or bafA (Figure 4A), make lysosomal cell death induced by GA101 in CLL cells likely. Golay et al recently proposed that type II anti-CD20–induced cell death detected by flow cytometry is an artifact of HA.[46] An argument against this hypothesis is the prominent cell death inhibition by concA in the presence of HA, as has also been observed with cathepsin inhibitors in some circumstances.[22,46] An interesting observation was the increased LysoTracker signal in the absence of HA in CD40-stimulated CLL cells incubated with GA101 plus cytoD. This suggests that the process of actin polymerization, HA, and increased lysosomal number and activity are not functionally linked. We therefore hypothesize that for GA101-induced LMP, and thus cell death, both HA and an increase in lysosomal volume and number are required. Indeed, a direct relationship between HA and cell death is not found for every mAb. For example, the pan-HLA mAb A9-1 induced high levels of HA but relatively low levels of cell death in Raji cells.[22] We found that CD40 stimulation increases the number and activity of lysosomes in CLL cells (as shown by an increase in LysoTracker signal, number of lysosomes, and lysosomal hydrolases cathepsin B and active GBA), thereby sensitizing them to GA101-induced lysosomal cell death.[47]

In comparison, RXL-induced cell death was not blocked in the presence of concA (Figure 4A) and induced no increase in lysosomal number or activity (Figure 5F), suggesting a different cell death mechanism. Indeed, we recently showed that RXL induces ROS-dependent cell death in CD40-stimulated CLL cells,[23] whereas this was not observed with GA101 (Figure 5E). Therefore, the basis for the death-inducing capacity of the type I CD20 mAb rituximab seems to be quite different from that of GA101. Table 3 summarizes the differences between rituximab- and GA101-induced cell death in CD40-stimulated CLL cells. GA101 induces strong HA and lysosomal-dependent cell death, whereas RXL induces Ca^{2+}- and ROS-dependent cell death. Both CD20 mAbs

Table 3. Summary of characteristics of RXL- and GA101-induced cell death in CD40-stimulated CLL cells

Characteristic	RXL	GA101
HA	+	++
LMP	−	+
Ca flux	+	−
ROS	+	−
MitoTracker	+	+
Annexin V/PI	+	+
Caspase activation	+	+
Sub-G_1	+	+

+ indicates present; ++, clearly present; and −, absent.

induce caspase activation as bystander phenomena of a different cell death mechanism. Cell death can be observed with annexin V/PI staining, as well as with MitoTracker staining and DNA fragmentation.

In Figure 7 we summarize our findings for GA101-induced lysosomal cell death in CD40 stimulated CLL cells, with inclusion of the indirect caspase activation. Anti-CD20–induced cell death is generally believed to be caspase independent[48-50]; however, some studies have shown that caspase activation plays a role.[13,50,51] In the present study, GA101 induced incomplete caspase-3 activation as measured by FACS and no full processing of caspase-3 was found by Western blot. Furthermore, no correlation between the amount of caspase activation and the percentage of dead cells was found. These results suggest at best a partial processing of caspase-3 during anti-CD20–induced cell death. Finally, GA101-induced cell death was not blocked by pan-caspase inhibitors, suggesting the participation of caspase-independent, nonclassic apoptosis. Cleavage of caspases has also been described in lysosomal cell death. The release of lysosomal proteases into the cytosol is directly involved in the cleavage of proapoptotic substrates and/or activation of caspases. This latter process is usually mediated indirectly through a cascade in which LMP causes the proteolytic activation of Bid[52] (which is cleaved by the 2 lysosomal cathepsins B and D), which then induces mitochondrial outer membrane permeabilization, resulting in cytochrome c release and apoptosome-dependent caspase activation (for review, see Boya and Kroemer[45]). This sequence of events is likely to occur in CD40-stimulated CLL cells after incubation with GA101 and could therefore be the result of lysosomal cell death and not reflect classic apoptosis. The identity of the responsible lysosomal hydrolase(s) is not certain. We applied various inhibitors of cathepsins, but were unable to prevent GA101-induced cell death in CLL cells (data not shown).

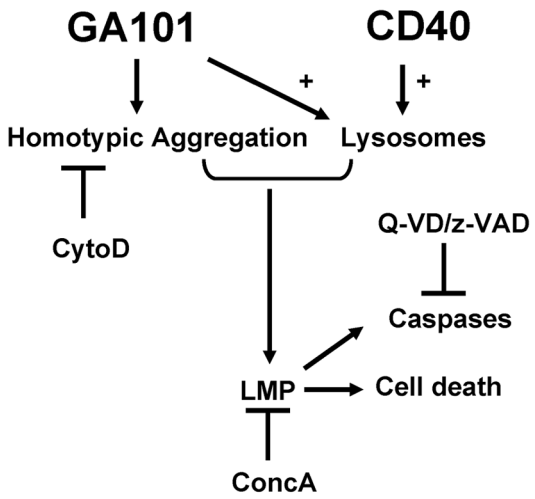

Figure 7. Model for GA101-induced cell death in CD40-stimulated CLL cells. GA101 induces HA, which can be blocked by cytoD. CD40 stimulation increases the number of lysosomes that are susceptible to swelling and burst via GA101 engagement. Both GA101-induced HA and an increase in lysosomal number are required to result in LMP, leading to cell death. An increase in lysosomal volume and LMP can be inhibited by concA. Release of cathepsins into the cytosol after LMP leads to caspase activation. Caspase activation, but not cell death, is inhibited by Z-VAD and Q-VD.

We tested the effect of GA101 in combination with cytotoxic drugs in CD40-stimulated, drug-resistant CLL cells with mutated and unmutated IGHV genes and in p53-dysfunctional CLL cells. As expected, p53-dysfunctional CLL cells were insensitive to chlorambucil, fludarabine, and nutlin all of which have a p53-dependent mode of action. However, these cells were partially sensitive to bendamustine (supplemental Figure 1). The mechanism of action of bendamustine has been principally linked to p53 stabilization; however, a recent study showed that bendamustine cytotoxicity in CLL cells was p53 independent and mediated by ROS generation and triggering of the intrinsic apoptotic pathway,[53,54] which fits well with our data. We observed an 80%-100% cell death induction in drug-resistant CLL cells and in patients with p53-dysfunctional CLL cells by combining GA101 with cytotoxic drugs. The latter finding is of particular importance because these patients do not respond to conventional therapy and tend to have a rapidly progressive disease.[55] Moreover, the frequency of p53 dysfunction increases to nearly 50% as the disease progresses and after therapy.[9,10] We have shown previously that RXL also induces cell death in p53-dysfunctional CLL cells.[23] Combining RXL, G, or GXL with cisplatin or fludarabine results in strong cell death induction at low concentrations of cytostatic drugs (Figure 7B).[23] The results of the present study provide a rationale for combining cytotoxic drugs with type II anti-CD20 mAbs for the treatment of CLL.

Acknowledgments

The authors are indebted to the participating CLL patients for their commitment to this study.

Authorship

Contribution: M.J. designed the research, performed the experiments, analyzed the data and wrote the manuscript; G.G.W.v.B., W.W.K., and J.M.T. performed the experiments and analyzed the data; E.A.R. designed and helped with the confocal experiments; C.K. and P.U. contributed the new mAb GA101 and designed the research; R.A.W.v.L. and M.H.J.v.O. designed the research and analyzed the data; and E.E. designed the research, analyzed the data, and wrote the manuscript.

Conflict-of-interest disclosure: C.K. and P.U. are employed by and have equity ownership and patents and royalties with Roche. The remaining authors declare no competing financial interests.

The current affiliation for R.A.W.v.L. is Sanquin Blood Supply, Amsterdam, The Netherlands.

Correspondence: M. Jak, Academic Medical Center, Department of Hematology, Meibergdreef 9, 1105 AZ Amsterdam, The Netherlands; e-mail: m.jak@amc.uva.nl.

References

1. Burger JA, Ghia P, Rosenwald A, Caligaris-Cappio F. The microenvironment in mature B-cell malignancies: a target for new treatment strategies. *Blood.* 2009;114(16):3367-3375.
2. Furman RR, Asgary Z, Mascarenhas JO, Liou HC, Schattner EJ. Modulation of NF-kappa B activity and apoptosis in chronic lymphocytic leukemia B cells. *J Immunol.* 2000;164(4):2200-2206.
3. Hallaert DY, Jaspers A, van Noesel CJ, et al. c-Abl kinase inhibitors overcome CD40-mediated drug resistance in CLL: implications for therapeutic targeting of chemoresistant niches. *Blood.* 2008;112(13):5141-5149.
4. Kater AP, Evers LM, Remmerswaal EB, et al. CD40 stimulation of B-cell chronic lymphocytic leukaemia cells enhances the anti-apoptotic profile, but also Bid expression and cells remain susceptible to autologous cytotoxic T-lymphocyte attack. *Br J Haematol.* 2004;127(4):404-415.
5. Romano MF, Lamberti A, Tassone P, et al. Triggering of CD40 antigen inhibits fludarabine-induced apoptosis in B chronic lymphocytic leukemia cells. *Blood.* 1998;92(3):990-995.
6. Vogler M, Butterworth M, Majid A, et al. Concurrent up-regulation of BCL-XL and BCL2A1 induces approximately 1000-fold resistance to ABT-737 in chronic lymphocytic leukemia. *Blood.* 2009;113(18):4403-4413.
7. Caligaris-Cappio F. Role of the microenvironment in chronic lymphocytic leukaemia. *Br J Haematol.* 2003;123(3):380-388.
8. Ghia P, Caligaris-Cappio F. The indispensable role of microenvironment in the natural history of low-grade B-cell neoplasms. *Adv Cancer Res.* 2000;79:157-173.
9. Lozanski G, Heerema NA, Flinn IW, et al. Alemtuzumab is an effective therapy for chronic lymphocytic leukemia with p53 mutations and deletions. *Blood.* 2004;103(9):3278-3281.
10. Sturm I, Bosanquet AG, Hermann S, et al. Mutation of p53 and consecutive selective drug resistance in B-CLL occurs as a consequence of prior DNA-damaging chemotherapy. *Cell Death Differ.* 2003;10(4):477-484.
11. Hallek M, Fischer K, Fingerle-Rowson G, et al. Addition of rituximab to fludarabine and cyclophosphamide in patients with chronic lymphocytic leukaemia: a randomised, open-label, phase 3 trial. *Lancet.* 2010;376(9747):1164-1174.
12. Robak T, Dmoszynska A, Solal-Celigny P, et al. Rituximab plus fludarabine and cyclophosphamide prolongs progression-free survival compared with fludarabine and cyclophosphamide alone in previously treated chronic lymphocytic leukemia. *J Clin Oncol.* 2010;28(10):1756-1765.
13. Deans JP, Li H, Polyak MJ. CD20-mediated apoptosis: signalling through lipid rafts. *Immunology.* 2002;107(2):176-182.
14. Glennie MJ, French RR, Cragg MS, Taylor RP. Mechanisms of killing by anti-CD20 monoclonal antibodies. *Mol Immunol.* 2007;44(16):3823-3837.
15. Mössner E, Brunker P, Moser S, et al. Increasing the efficacy of CD20 antibody therapy through the engineering of a new type II anti-CD20 antibody with enhanced direct- and immune effector cell-mediated B-cell cytotoxicity. *Blood.* 2010;115(22):4393-4402.
16. Walshe CA, Beers SA, French RR, et al. Induction of cytosolic calcium flux by CD20 is dependent upon B Cell antigen receptor signaling. *J Biol Chem.* 2008;283(25):16971-16984.
17. Coiffier B, Lepretre S, Pedersen LM, et al. Safety and efficacy of ofatumumab, a fully human monoclonal anti-CD20 antibody, in patients with relapsed or refractory B-cell chronic lymphocytic leukemia: a phase 1-2 study. *Blood.* 2008;111(3):1094-1100.
18. Niederfellner G, Lammens A, Mundigl O, et al. Epitope characterization and crystal structure of GA101 provide insights into the molecular basis for type I/II distinction of CD20 antibodies. *Blood.* 2011;118(2):358-367.
19. Patz M, Isaeva P, Forcob N, et al. Comparison of the in vitro effects of the anti-CD20 antibodies rituximab and GA101 on chronic lymphocytic leukaemia cells. *Br J Haematol.* 2011;152(3):295-306.
20. Morschhauser F, Cartron G, Lamy T, et al. Phase 1 study of RO5072759 (GA101) in relapsed/refractory chronic lymphocytic leukemia [Abstract]. *Blood.* 2009;114(suppl 1):884.
21. Alduaij W, Ivanov A, Honeychurch J, et al. Novel type II anti-CD20 monoclonal antibody (GA101) evokes homotypic adhesion and actin-dependent, lysosome-mediated cell death in B-cell malignancies. *Blood.* 2011;117(17):4519-4529.
22. Ivanov A, Beers SA, Walshe CA, et al. Monoclonal antibodies directed to CD20 and HLA-DR can elicit homotypic adhesion followed by lysosome-mediated cell death in human lymphoma and leukemia cells. *J Clin Invest.* 2009;119(8):2143-2159.
23. Jak M, van Bochove GG, van Lier RA, Eldering E, van Oers MH. CD40 stimulation sensitizes CLL cells to rituximab-induced cell death. *Leukemia.* 2011;25(6):968-978.
24. Mous R, Savage P, Remmerswaal EB, et al. Redirection of CMV-specific CTL towards B-CLL via CD20-targeted HLA/CMV complexes. *Leukemia.* 2006;20(6):1096-1102.
25. Mackus WJ, Kater AP, Grummels A, et al. Chronic lymphocytic leukemia cells display p53-dependent drug-induced Puma upregulation. *Leukemia.* 2005;19(3):427-434.
26. Witte MD, Kallemeijn WW, Aten J, et al. Ultrasensitive in situ visualization of active glucocerebrosidase molecules. *Nat Chem Biol.* 2010;6(12):907-913.
27. Koopman G, Reutelingsperger CP, Kuijten GA, et al. Annexin V for flow cytometric detection of phosphatidylserine expression on B cells undergoing apoptosis. *Blood.* 1994;84(5):1415-1420.
28. Krishan A. Rapid flow cytofluorometric analysis of mammalian cell cycle by propidium iodide staining. *J Cell Biol.* 1975;66(1):188-193.
29. Kaspers GJ, Veerman AJ, Pieters R, et al. Drug combination testing in acute lymphoblastic leukemia using the MTT assay. *Leuk Res.* 1995;19(3):175-181.
30. Tonino SH, van GM, Eldering E, van Oers MH, Kater AP. R-DHAP is effective in fludarabine-refractory chronic lymphocytic leukemia. *Leukemia.* 2010;24(3):652-654.
31. Hallaert DY, Spijker R, Jak M, et al. Crosstalk among Bcl-2 family members in B-CLL: seliciclib acts via the Mcl-1/Noxa axis and gradual exhaustion of Bcl-2 protection. *Cell Death Differ.* 2007;14(11):1958-1967.
32. Lazebnik YA, Kaufmann SH, Desnoyers S, Poirier GG, Earnshaw WC. Cleavage of poly(ADP-ribose) polymerase by a proteinase with properties like ICE. *Nature.* 1994;371(6495):346-347.
33. Tromp JM, Tonino SH, Elias JA, et al. Dichotomy in NF-kappaB signaling and chemoresistance in immunoglobulin variable heavy-chain-mutated versus unmutated CLL cells upon CD40/TLR9 triggering. *Oncogene.* 2010;29(36):5071-5082.
34. Kansas GS, Tedder TF. Transmembrane signals generated through MHC class II, CD19, CD20, CD39, and CD40 antigens induce LFA-1-dependent and independent adhesion in human B cells through a tyrosine kinase-dependent pathway. *J Immunol.* 1991;147(12):4094-4102.
35. Behr SI, Korinth D, Schriever F. Differential adhesion pattern of B cell chronic lymphocytic leukemia cells. *Leukemia.* 1998;12(1):71-77.
36. Muroi M, Shiragami N, Nagao K, Yamasaki M, Takatsuki A. Folimycin (concanamycin A), a specific inhibitor of V-ATPase, blocks intracellular translocation of the glycoprotein of vesicular stomatitis virus before arrival to the Golgi apparatus. *Cell Struct Funct.* 1993;18(3):139-149.
37. Kroemer G, Jaattela M. Lysosomes and autophagy in cell death control. *Nat Rev Cancer.* 2005;5(11):886-897.
38. Steele AJ, Prentice AG, Hoffbrand AV, et al. p53-mediated apoptosis of CLL cells: evidence for a transcription-independent mechanism. *Blood.* 2008;112(9):3827-3834.
39. Rosenwald A, Chuang EY, Davis RE, et al. Fludarabine treatment of patients with chronic lymphocytic leukemia induces a p53-dependent gene expression response. *Blood.* 2004;104(5):1428-1434.
40. Saha MN, Micallef J, Qiu L, Chang H. Pharmacological activation of the p53 pathway in haematological malignancies. *J Clin Pathol.* 2010;63(3):204-209.
41. Secchiero P, Barbarotto E, Tiribelli M, et al. Functional integrity of the p53-mediated apoptotic pathway induced by the nongenotoxic agent nutlin-3 in B-cell chronic lymphocytic leukemia (B-CLL). *Blood.* 2006;107(10):4122-4129.
42. Strauss SJ, Higginbottom K, Juliger S, et al. The proteasome inhibitor bortezomib acts independently of p53 and induces cell death via apoptosis and mitotic catastrophe in B-cell lymphoma cell lines. *Cancer Res.* 2007;67(6):2783-2790.
43. Tonino SH, van LJ, van Oers MH, et al. ROS-mediated upregulation of Noxa overcomes chemoresistance in chronic lymphocytic leukemia. *Oncogene.* 2011;30(6):701-713.
44. Kater AP, van Oers MH, Kipps TJ. Cellular immune therapy of chronic lymphocytic leukemia. *Blood.* 2007;110(8):2811-2818.
45. Boya P, Kroemer G. Lysosomal membrane permeabilization in cell death. *Oncogene.* 2008;27(50):6434-6451.
46. Golay J, Bologna L, Andre PA, et al. Possible misinterpretation of the mode of action of therapeutic antibodies in vitro: homotypic adhesion and flow cytometry result in artefactual direct cell death. *Blood.* 2010;116(17):3372-3373.
47. Ono K, Kim SO, Han J. Susceptibility of lysosomes to rupture is a determinant for plasma membrane disruption in tumor necrosis factor alpha-induced cell death. *Mol Cell Biol.* 2003;23(2):665-676.
48. Cragg MS, Glennie MJ. Antibody specificity controls in vivo effector mechanisms of anti-CD20 reagents. *Blood.* 2004;103(7):2738-2743.
49. Daniels I, Abulayha AM, Thomson BJ, Haynes AP. Caspase-independent killing of Burkitt lymphoma cell lines by rituximab. *Apoptosis.* 2006;11(6):1013-1023.
50. van der Kolk LE, Evers LM, Omene C, et al. CD20-induced B cell death can bypass mitochondria and caspase activation. *Leukemia.* 2002;16(9):1735-1744.
51. Ghetie MA, Bright H, Vitetta ES. Homodimers but not monomers of Rituxan (chimeric anti-CD20) induce apoptosis in human B-lymphoma cells and synergize with a chemotherapeutic agent and an immunotoxin. *Blood.* 2001;97(5):1392-1398.
52. Cirman T, Oresic K, Mazovec GD, et al. Selective disruption of lysosomes in HeLa cells triggers apoptosis mediated by cleavage of Bid by multiple papain-like lysosomal cathepsins. *J Biol Chem.* 2004;279(5):3578-3587.
53. Dennie TW, Kolesar JM. Bendamustine for the treatment of chronic lymphocytic leukemia and rituximab-refractory, indolent B-cell non-Hodgkin lymphoma. *Clin Ther.* 2009;31 (pt 2):2290-2311.
54. Roué G, Lopez-Guerra M, Milpied P, et al. Bendamustine is effective in p53-deficient B-cell neoplasms and requires oxidative stress and caspase-independent signaling. *Clin Cancer Res.* 2008;14(21):6907-6915.
55. Döhner H, Stilgenbauer S, Benner A, et al. Genomic aberrations and survival in chronic lymphocytic leukemia. *N Engl J Med.* 2000;343(26):1910-1916.